Anti-atherogenic effects of resveratrol via liver X receptor α-dependent upregulation of ATP-binding cassette transporters A1 and G1 in macrophages

Chun-Yu Chang[a], Tsung-Han Lee[b,c,], Wayne H-H Sheu[a,d,e,f,*]*

[a]*Graduate Institute of Biomedical Sciences, National Chung Hsing University, Taichung, Taiwan*
[b]*Department of Life Sciences, National Chung Hsing University, Taichung, Taiwan*
[c]*Department of Biological Science and Technology, China Medical University, Taichung, Taiwan*
[d]*Division of Endocrinology and Metabolism, Department of Internal Medicine, Taichung Veterans General Hospital, Taichung, Taiwan*
[e]*School of Medicine, National Yang Ming University, Taipei, Taiwan*
[f]*School of Medicine, National Defense Medical Center, Taipei, Taiwan*

ARTICLE INFO

ABSTRACT

Resveratrol (RSV), a phenolic component, is found in grape skins, peanuts, pistachios and red wine. RSV has protective activities in atherosclerosis, yet the detailed mechanisms are not fully elucidated. In the present study, we observed that RSV inhibited oxLDL-mediated lipid accumulation through the enhancement of cholesterol efflux in THP-1-derived macrophages and explored the possible underlying mechanisms. RSV dose-dependently enhanced the mRNA and protein levels of ATP-binding membrane cassette transporters A1 and G1 (ABCA1 and ABCG1) but had no effect on the mRNA expression of scavenger receptor class BI (SR-BI) in cholesterol homeostasis. Additionally, the functional inhibition of ABCA1 and ABCG1 with short hairpin RNA abrogated the effects of RSV on lipid accumulation. The upregulation of ABCA1 and ABCG1 by RSV depended on LXRα, as evidenced by an increase in the nuclear levels of LXRα through the induction of nuclear translocation. The functional inhibition of LXRα with a pharmacological inhibitor, geranylgeranyl pyrophosphate (GGPP), abolished the RSV-mediated protective effects in macrophages. These findings suggest that LXRα-dependent upregulation of ABCA1 and ABCG1 might mediate the beneficial effects of RSV, which ameliorated the oxLDL-mediated lipid accumulation in the process of lipid-laden foam cells formation.

1. Introduction

Atherosclerosis is a major cause of cardiovascular disease (CVD) and is dependent on the increase of circulating cholesterol levels and inflammation in the vascular wall. Cholesterol homeostasis by macrophages is critical for the initiation and progression of atherosclerotic lesions (Li & Glass, 2002). Formation of foam cell is mainly due to uncontrolled uptake of modified low-density lipoprotein (LDL) or impaired cholesterol efflux in macrophages. This result in

* *Corresponding authors.* Addresses: Department of Life Sciences, National Chung Hsing University, Taichung, 250 Kuo-Kuang Road, Taichung 402, Taiwan. Tel.: +886 4 22856141; fax: +886 4 22874740 (T.-H. Lee), Division of Endocrinology and Metabolism, Department of Internal Medicine, Taichung Veterans General Hospital, No. 160, Sec. 3, Taichung-Kang Road, Taichung 407, Taiwan. Tel.: +886 4 23741340; fax: +886 4 23595046 (W.H.-H. Sheu).
   E-mail addresses: thlee@email.nchu.edu.tw (T.-H. Lee), whhsheu@vghtc.gov.tw (W.H-H Sheu).

an excessive level of lipoprotein-derived cholesterol, which is consequently processed, stored and accumulated inside the cells (Takahashi, Takeya, & Sakashita, 2002). High-density lipoprotein (HDL) plays a crucial role in removing excess cholesterol in atherosclerotic plaques, and transporting it back to the liver by reverse cholesterol transport (RCT) (Cuchel & Rader, 2006; Linsel-Nitschke & Tall, 2005; de Winther & Hofker, 2000). The efflux of intracellular cholesterol in macrophages is mediated by RCT transporters (RCTs), including scavenger receptors (SRs), class B type I (SR-BI) and the ATP-binding cassette transporters, A1 and G1 (ABCA1 and ABCG1) (Ji et al., 1997; Wang, Lan, Chen, Matsuura, & Tall, 2004; Yokoyama, 2005). Ample evidence has demonstrated that the dietary supplementation with antioxidants regulates the expression of SRs or RCTs, leading to the suppression of cholesterol accumulation in macrophages and the prevention of CVD (Kaliora, Dedoussis, & Schmidt, 2006). Furthermore, accumulating evidence suggests that the mortality due to CVD is lowered by a moderate consumption of red wine (Bhavnani, Cecutti, Gerulath, Woolever, & Berco, 2001; Renaud & de Lorgeril, 1992).

Resveratrol (trans-3, 4, 5-trihydroxystilbene, RSV), a polyphenol component of *Vitis vinifera* L, is mainly found in grapes, grape-derived products and a few other plant species, including peanuts, pistachios and berries. RSV was found to be abundant in the skin of grapes and present in higher concentrations in red wines (Kopp, 1998), and previous studies revealed that RSV exhibited many beneficial effects against CVD (Bhat, Kosmeder, & Pezzuto, 2001). The cardioprotection conferred by RSV may be due to its multiple functions that act on different cellular targets, including the inhibition of LDL oxidation, suppression of platelet aggregation, and inhibition of smooth muscle and endothelial cell proliferation and peroxidation (Poussier, Cordova, Becquemin, & Sumpio, 2005; Wang et al., 2002). Indeed, studies on the consumption of red wine have shown increased HDL levels (Araya, Rodrigo, Orellana, & Rivera, 2001) or decreased LDL cholesterol levels in the plasma (Zou et al., 2000), and over recent decades, evidence suggested various benefits of RSV, including anti-diabetes, life extension, attenuation of the inflammatory response in macrophages, and anti-atherosclerosis, in both humans and experimental animals (Agarwal & Baur, 2011; Berrougui, Grenier, Loued, Drouin, & Khalil, 2009; Borra, Smith, & Denu, 2005; Cullen et al., 2007; Zhang et al., 2010). Additionally, RSV has been shown to enhance the expression and activity of endothelial nitric oxide synthase, block the TNFα-induced adhesion of monocytes and granulocytes to endothelial cells, and protect against oxidized LDL (oxLDL)-induced cytotoxicity in endothelial cells (Ferrero et al., 1998; Manna, Mukhopadhyay, & Aggarwal, 2000; Ou et al., 2006; Wallerath et al., 2002). These results suggested that RSV has multiple protective cardiovascular and related physiological functions. However, the effects of RSV on macrophage foam cell formation and intracellular cholesterol metabolism remain unexplored. The aim of the present study was to investigate whether RSV inhibits the formation of foam cells and to determine the involved molecular mechanism.

We first examined the effects of RSV on oxLDL-induced foam cell formation. Second, we investigated the effects of RSV on the expression of SR-BI, ABCA1 and ABCG1. Third,

we explored the molecular mechanisms involved in the RSV-mediated modulation of lipid accumulation. Our results demonstrated that RSV suppressed oxLDL-mediated lipid accumulation and upregulated LXRα and its target genes (ABCA1 and ABCG1) in a dose- and time-dependent manner in THP-1 monocyte-derived macrophages.

2.   Materials and methods

2.1.   Chemicals and antibodies

Resveratrol (RSV), T0901317, phorbol 12-myristate 13-acetate (PMA), geranylgeranyl pyrophosphate (GGPP), and Oil-red O were purchased from Sigma (St. Louis, MO, USA). The 2× SYBR Green PCR Master Mix was obtained from Bio-Rad (Hercules, CA, USA). The cholesterol assay kit was obtained from BioVision (Mountain View, CA, USA). 3-Dodecanoyl-NBD-cholesterol and the thiobarbituric acid-reactive substance (TBARS) assay kit were acquired from Cayman (Michigan, MS, USA). RPMI 1640 medium, Lipofectamine™ 2000, DAPI and AlexaFluor-488-conjugated donkey anti-goat IgG were procured from Invitrogen (Auckland, NY, USA), the primary antibodies against ABCA1 (ab18180), ABCG1 (ab52617) and LXRα (ab41902) were purchased from Abcam (Cambridge, MA, USA) and SR-BI (sc-32342) and α-tubulin (sc-5286) were bought from Santa Cruz Biotechnology (Santa Cruz, CA, USA). All other chemicals were of analytical grade or purer.

2.2.   Cell culture

THP-1 cells, a human acute monocytic leukemia cell line (ATCC TIB-202), were cultured in RPMI 1640 medium supplemented with 10% fetal bovine serum (FBS), 100 μg/ml penicillin, and 100 μg/ml streptomycin at 37 °C in a 5% CO_2 atmosphere. Before experiments, the cells were differentiated for 72 h with 50 ng/ml PMA. Total RNA was prepared from THP-1 cells plated in dishes at a density of 5×10^5 cells. Protein extracts were prepared from cells cultured at a density of 10^7. For the Oil-red O stain and immunofluorescence assay, the THP-1 cells were seeded on coverslips at a density of 4×10^5 cells.

2.3.   Lipoprotein separation and oxidation

The methods were modified from Ou et al. (2006). Native LDL isolated from fresh normolipidemic human serum by sequential ultracentrifugation (ρ = 1.019–1.063 g/ml). Cu^{2+}-modified LDL was prepared by the exposure of the LDL to 10 μM $CuSO_4$ for 24 h at 37 °C. The extent of oxidation was monitored using a TBARS assay, following the manufacturer's instructions. OxLDL containing approximately 30–60 nm of TBARS (defined as malondialdehyde equivalents per milligram of LDL protein) was used for experiments.

2.4.   Resveratrol preparation

RSV was dissolved in DMSO. Untreated control cells were given the corresponding amount of DMSO that was used for the highest RSV concentration.

2.5. RNA extraction and real-time PCR

Total RNA was extracted using RNA-Bee™ (Tel-Test, Friendwood, TX, USA) following the manufacturer's instructions. The first-strand cDNA was synthesized using a SuperScript III reverse transcriptase kit (Invitrogen, Auckland, NY, USA). Each PCR contained 100 ng of cDNA, 10 μl 2× SYBR Green PCR Master Mix, and 10 μM of an optimized human ABCA1, ABCG1, SR-B1 and GAPDH-specific primer pair, respectively. Quantitative PCR was performed with an Mini Opticon real-time PCR system (Bio-Rad, Hercules, CA, USA) under thermal cycling (10 min at 95 °C and then 40 cycles of 95 °C for 15 s, 60 °C for 30 s, and 72 °C for 30 s). Sequences are shown in the Supplementary Table 1. Relative quantification was performed using the comparative cycle threshold (C_T) method, as recommended by the manufacturer. All quantifications are normalized to an endogenous control for GAPDH. All samples were run in triplicate. The data were analyzed by the Bio-Rad CFX manager software.

2.6. Preparation of nuclear extracts

Cells were suspended in 50 μl buffer containing 10 mM 4-(2-hydroxyethyl)-1- piperazineethanesulfonic acid (HEPES) (pH 7.9), 1.5 mM $MgCl_2$, 10 mM KCl, 0.5 mM Dithiothreitol (DTT) and 0.5 mM henylmethanesulfonylfluoride (PMSF) and then vortexed for 15 s and allowed to stand at 4 °C for 10 min. The cell suspension was subsequently centrifuged at 12,000g for 5 min at 4 °C, and the supernatants were used as the cytoplasmatic extracts. The pellets were resuspended in 30 μl buffer containing 20 mM HEPES (pH 7.9), 25% glycerol, 420 mM NaCl, 1.5 mM $MgCl_2$, 0.2 mM ethylenediaminetetraacetic acid (EDTA), 0.5 mM DTT, and 0.5 mM PMSF and incubated for 30 min on ice. After 10 min centrifugation at 18,000g the nuclear extracts were collected from the supernatant.

2.7. Western blotting

Treated and untreated cells were lysed with RIPA buffer (98% PBS, 1% Igepal CA-630, 0.1% SDS, 0.5% sodium deoxycholate and protease inhibitor cocktail). The cell lysates were centrifuged at 12,000g for 10 min at 4 °C. The supernatants were collected and the BCA protein assay reagents (Pierce, Rockford, IL, USA) were used to determine the protein content using BSA (Sigma, St. Louis, MO, USA) as the standard. Immunoblotting was performed according to protocol of Sevov, Elfineh, & Cavelier, 2006. The luminescent signal was detected using the Gel Doc XR+ image system (Bio-Rad, Hercules, CA, USA), and the images were exported using Image lab software (Bio-Rad). α-Tubulin were used as the internal control.

2.8. Immunofluorescence assay

Cells seeded on coverslips were treated with 20 μM RSV for 6 h and then fixed in 4% paraformaldehyde and permeabilized with 0.1% Triton X-100. Subsequently, the cells were incubated with the polyclonal anti-LXRα antibody (200× dilution) for 1 h and washed with 0.01% Triton X-100. The goat anti-rabbit IgG conjugated Alexa Fluor 488 was used to detect the primary LXRα antibody. The coverslips were mounted onto microscopy glass slide with mounting solution containing DAPI (Invitrogen) and observed using a confocal laser scanning microscope (FV2000, Olympus, Tokyo, Japan) with a 488 nm argon-ion laser.

2.9. Cytoplasmic lipid detection

2.9.1. Oil-red O staining
THP-1 cells were pre-treated with various concentrations RSV for 2 h and then stimulated with oxLDL for 24 h, which led to lipid accumulation, as revealed by the measurement of the intracellular lipid or cholesterol contents. Cells were fixed with 4% paraformaldehyde and then stained with 0.5% Oil-red O dye. Hematoxylin was used for the counterstaining. The density of the lipid content was evaluated by alcohol extraction after staining. The absorbance at 540 nm was measured using a microplate reader (VersaMax™, Molecular Devices, Sunnyvale, CA, USA).

2.9.2. Cholesterol measurement
Cellular cholesterol was extracted using of hexane/isopropanol (3:2, v/v). After removing the cellular debris, the supernatant was dried under nitrogen flush. The level of cholesterol was measured using a cholesterol assay kit, and the absorbance at 450 nm was measured using a microplate reader (VersaMax™).

2.9.3. Cholesterol efflux assay
Cells were treated with various concentrations of RSV for 12 h and then equilibrated with NBD-cholesterol (1 μg/ml) for an additional 6 h in the presence of RSV. Subsequently, the NBD-cholesterol-labeled cells were washed twice with PBS and incubated in RPMI 1640 medium for 6 h. The fluorescence-labeled cholesterol released from the cells into the medium was measured using a multilabel counter (PerkinElmer VICTOR3™ 1420, Waltham, MA, USA). The cholesterol efflux was expressed as the percentage fluorescence in the medium relative to the total fluorescence (cells and medium).

2.10. Transient transfection

ABCA1 and ABCG1 shRNAs (purchased from the Academia Sinica, Taipei, Taiwan) and the pLKO.1 scramble (Amp⁺) plasmid (a gift from Dr. Jeremy Jian-Wei Chen; Institute of Biomedical Science, National Chung Hsing University, Taichung, Taiwan) as a control were transfected into THP-1 cells using the Lipofectamine™ 2000 reagent. After 24 h following the transfection, the cells were treated with RSV or oxLDL for an additional 24 h and were then lysed for immunoblotting and Oil-red O staining. The cells stably transfected with ABCA1 or ABCG1 shRNA were maintained in a medium containing puromycin (10 μg/ml).

2.11. Statistical analysis

The results are shown as the means ± SEM (the standard error of the mean). In the time and dose analysis, statistical significance was determined using a Student's t-test compared to control. In the cytoplasmic lipid detection, statistical significance was determined using one-way analysis of variance

(ANOVA) followed by Dunnett's test. The lipid content by gene knockdown transfection experiments, different groups at the same time point were compared by one-way ANOVA followed by Tukey's pairwise method. Values ($P < 0.05$) were considered statistically significant.

3. Results

3.1. RSV attenuates oxidized LDL-induced lipid accumulation by increasing cholesterol efflux

To investigate the effects of RSV on oxLDL-induced foam cell formation, we treated THP-1 cells with various concentrations RSV and oxLDL, which led to lipid accumulation. The increase in lipid accumulation was markedly attenuated by the treatment with RSV in a dose-dependent manner (Fig. 1A–C). Additionally, the cholesterol efflux was evaluated by use of fluorescent NBD-cholesterol, and RSV dose-dependently increased the efficiency of cholesterol efflux in the macrophages (Fig. 1D).

3.2. RSV upregulates ABCA1 and ABCG1 expression in THP-1-derived macrophages

3.2.1. Determination of cytotoxicity
In order to establish a suitable working model of RSV in THP-1-derived macrophages, first, we treated THP-1 with various concentrations of RSV (0–100 μM) for 16 h. The cell viability was determined via MTT assay and showed that cell viability decreased with RSV concentration increasing (Supplementary Fig. 1). The relative cell viability was 81.2 and 39.75% at the concentration of 20 and 50 μM, respectively. To ensure authenticity, we decided to use 20 μM as the working concentration of RSV.

3.2.2. Time dependence
To explore the molecular mechanisms involved in the lipid-lowering effects of RSV, we examined the effects of RSV on the expression of SRs and RCTs. After treatment with a fixed starting concentration of RSV (20 μM), both the protein and mRNA levels of ABCA1 and ABCG1 were increased by time in the THP-1-derived macrophages. Other than ABCA1 and ABCG1, there was little effect on the expression level of SR-BI (Fig. 2A and B). Quantification the expression of mRNA was relied on real-time PCR.

3.2.3. Concentration dependence
THP-1 were treated with various concentrations of RSV (0, 1, 5, 10, 20, 50, and 100 μM) for 16 h. After treatment with RSV, both the protein and mRNA levels of ABCA1 and ABCG1 were dose-dependently upregulated in the macrophages (Fig. 3A and B). Upon the expression of SR-BI, the protein levels were influenced by RSV, and the mRNA expression was slightly but not significantly affected (Fig. 3B).
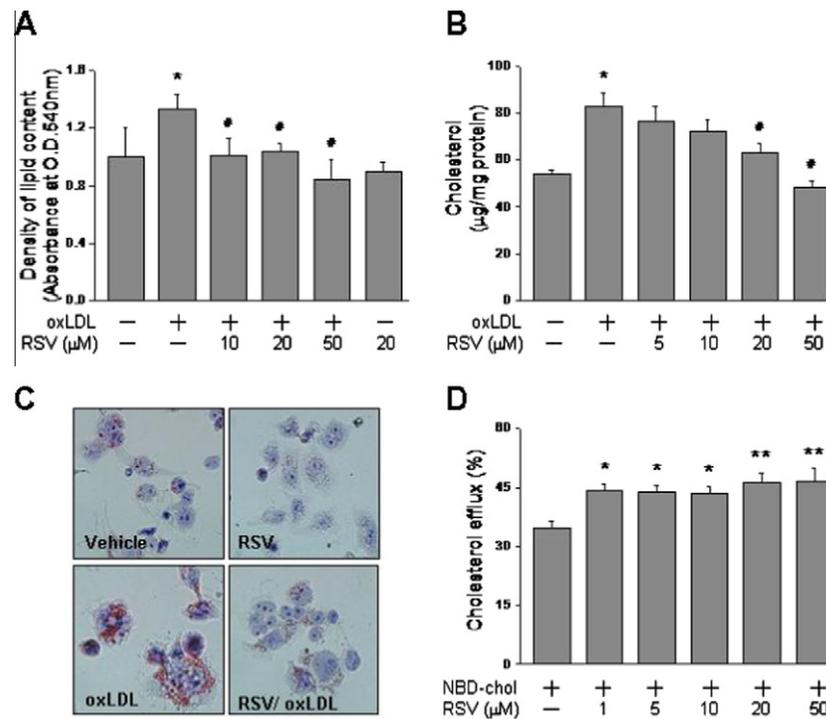
Fig. 1 – RSV attenuated lipid accumulation and promoted cholesterol efflux. THP-1-derived macrophages were pre-treated with the indicated concentrations of RSV (0–50 μM) for 2 h and were then stimulated with oxLDL (50 μg/ml) for 24 h. (A) RSV reduced lipid accumulation. The intracellular lipid quantified by Oil-red O stain. (B) RSV decreased cholesterol accumulation. The intracellular cholesterol quantified by an enzymatic method. (C) After staining with Oil-red O, the nuclei were stained with hematoxylin (objective: 40×). (D) RSV increased cholesterol efflux. Cholesterol efflux was expressed as the percentage of fluorescence in the medium relative to the total fluorescence. Data are the mean ± SEM ($n = 5$). Statistical significance at *$P < 0.05$ or **$P < 0.01$ compared with control; #$P < 0.05$ compared with oxLDL alone.
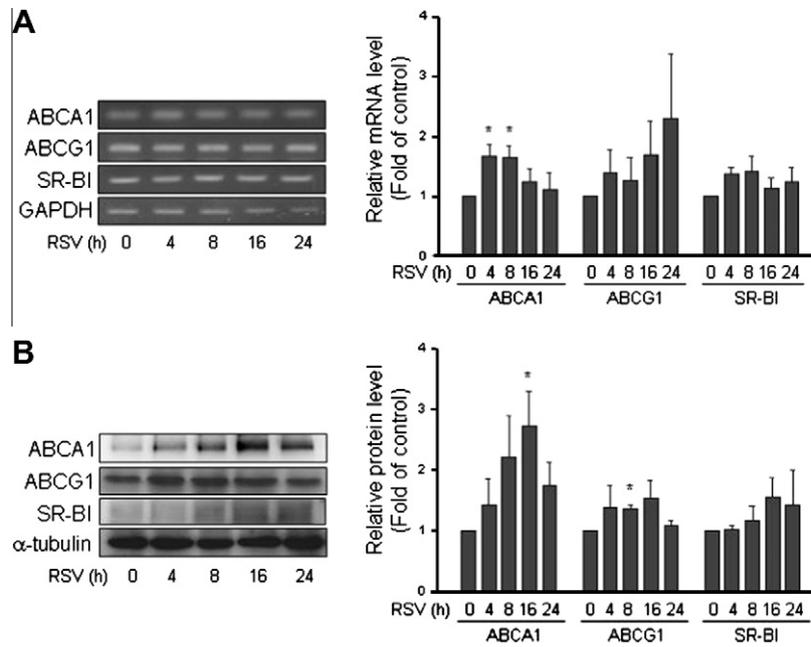
Fig. 2 – The effects of time course of RSV on the expression of ABCA1, ABCG1 and SR-BI. (A) The level of mRNA. (B) The level of protein. Macrophages were treated for the indicated time points (0–24 h). Data are the mean ± SEM ($n = 4$). Statistical significance at $^*P < 0.05$ compared with control.
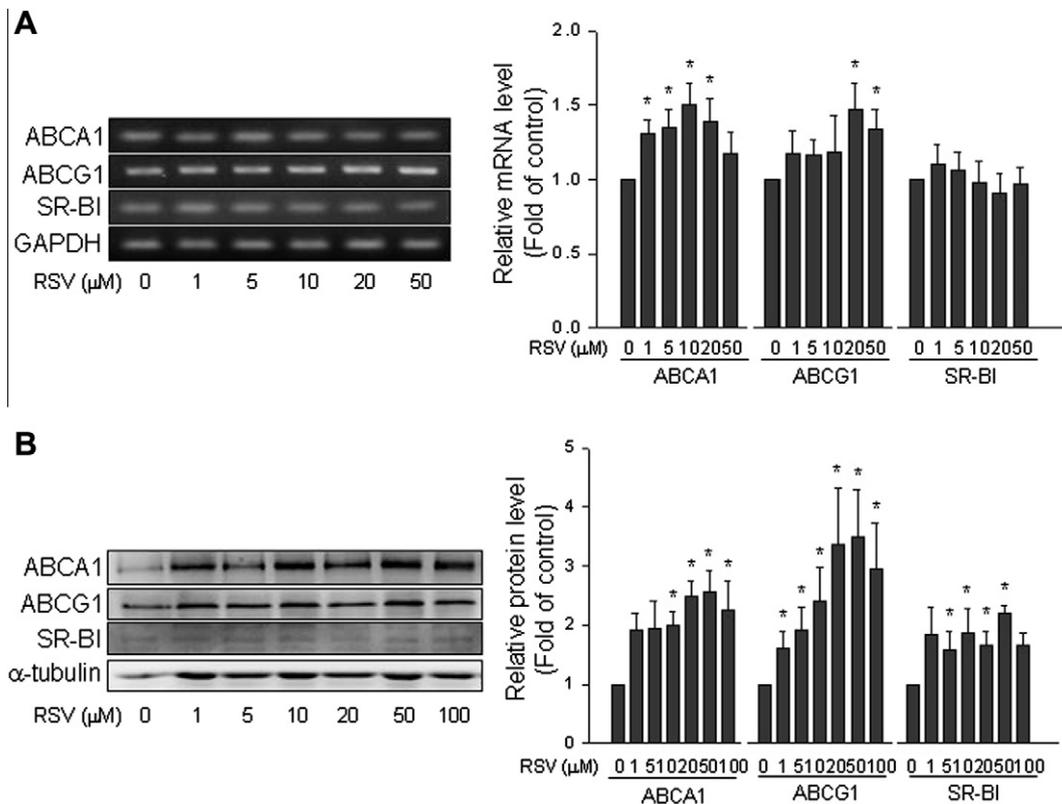
Fig. 3 – The effects dosage of RSV on the expression of ABCA1, ABCG1 and SR-BI. (A) The level of mRNA. (B) The level of protein. Macrophages were treated with the indicated dose (0–100 μM). Data are the mean ± SEM ($n = 5$). Statistical significance at $^*P < 0.05$ compared with control.

3.3. Functional inhibition of ABCA1 and ABCG1 with short hairpin RNA (shRNA) abrogated the effects of resveratrol on lipid accumulation

To clarify the role of ABCA1 and ABCG1 in maintaining cholesterol homeostasis, we transfected shRNA constructs (in pLKO.1 expression vectors) against ABCA1 or ABCG1 into THP-1. The protein levels of ABCA1 and ABCG1 were decreased in the gene knockdown macrophages compared to the wild-type macrophages (Fig. 4A and C). To determine the function of ABCA1 and ABCG1, we treated the macrophages with RSV and oxLDL, which led to lipid accumulation, as revealed by the measurement of the intracellular lipid or cholesterol contents. The suppression effects of RSV against intracellular lipid contents was totally abolished in ABCA1-KD or ABCG1-KD cells, even more than with oxLDL treatment alone (Fig. 4B, D).

3.4. RSV induces the nuclear translocation and activation of LXRα

The activation of the LXRα/RXR system has been suggested to play a critical role in regulating ABCA1 expression (Chawla et al., 2001; Sevov et al., 2006). To address whether LXRα is involved in the RSV-induced ABCA1 or ABCG1 upregulation, we examined the expression of LXRα in response to RSV treatment. The levels of LXRα in the nuclei were time-dependently increased with RSV treatment and the maximal expression of LXRα at 6 h (Fig. 5A). Confocal microscopic observations revealed that LXRα was distributed in both the nucleus and cytosol in the control cells but elevated translocated into the nucleus after RSV treatment (Fig. 5B).

3.5. Inhibition of LXRα activation abolished RSV-mediated gene expression of ABCA1 and ABCG1 and consequent lipid accumulation

To examine the roles of LXRα specifically, we performed additional experiments to demonstrate that the increase in ABCA1 and ABCG1 protein expression caused by RSV was mainly due to LXRα activation. The functional inhibition of LXRα by treatment with the LXRα-specific inhibitor, GGPP, diminished the effects of RSV and increased the protein expression of ABCA1 and ABCG1 (Fig. 5C). Moreover, the suppressive effects of RSV on the oxLDL-mediated lipid accumulation were completely abrogated under GGPP treatment (Fig. 5D).
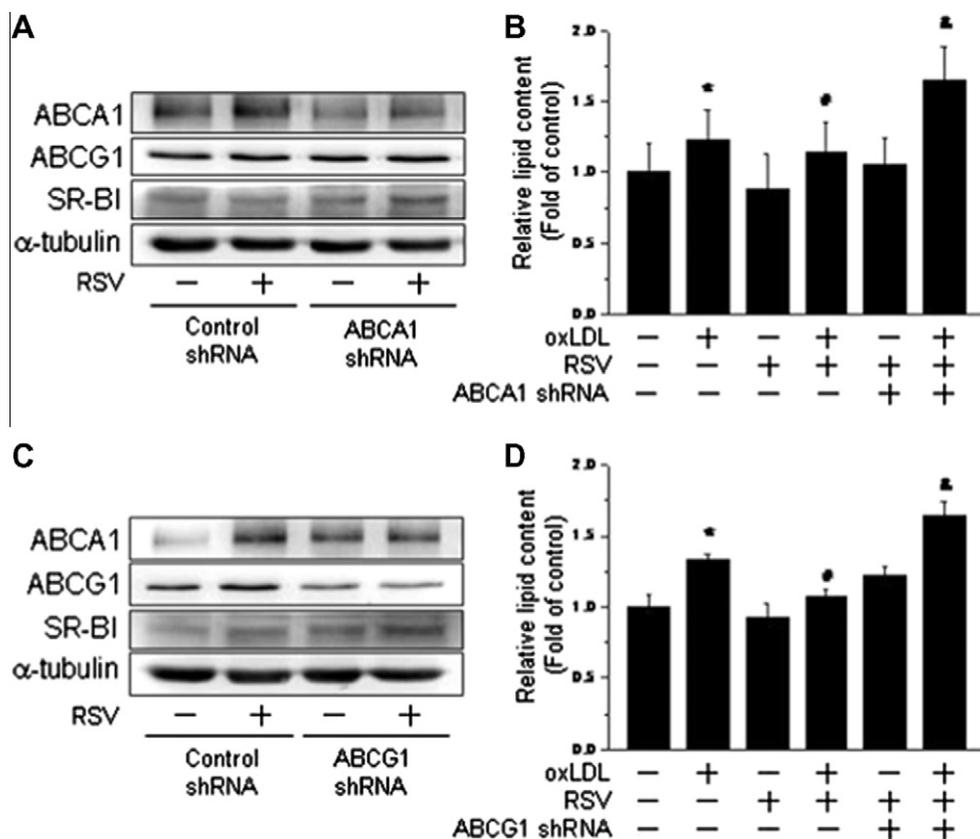
Fig. 4 – Knockdown of ABCA1 and ABCG1 expression diminished the resveratrol-mediated suppressive effects on lipid accumulation. Macrophages were transfected with 2 μg/ml shRNA of (A) ABCA1 or (C) ABCG1 for 24 h, and the cellular lysates were examined by western blot. (B and D) The suppression effects of RSV against intracellular lipid contents was totally abolished in ABCA1-KD or ABCG1-KD cells, even more than with oxLDL treatment alone. Macrophages were transfected with shRNA against ABCA1 or ABCG1 for 24 h and then treated with 20 μM RSV, 50 μg/ml oxLDL, or RSV/oxLDL for an additional 24 h. The intracellular lipid quantified by Oil-red O stain. Data are the mean ± SEM (n = 4). Statistical significance at *$P < 0.05$ compared with control; #$P < 0.05$ compared with RSV-treated alone; &$P < 0.05$ compared with RSV/oxLDL-treated group.
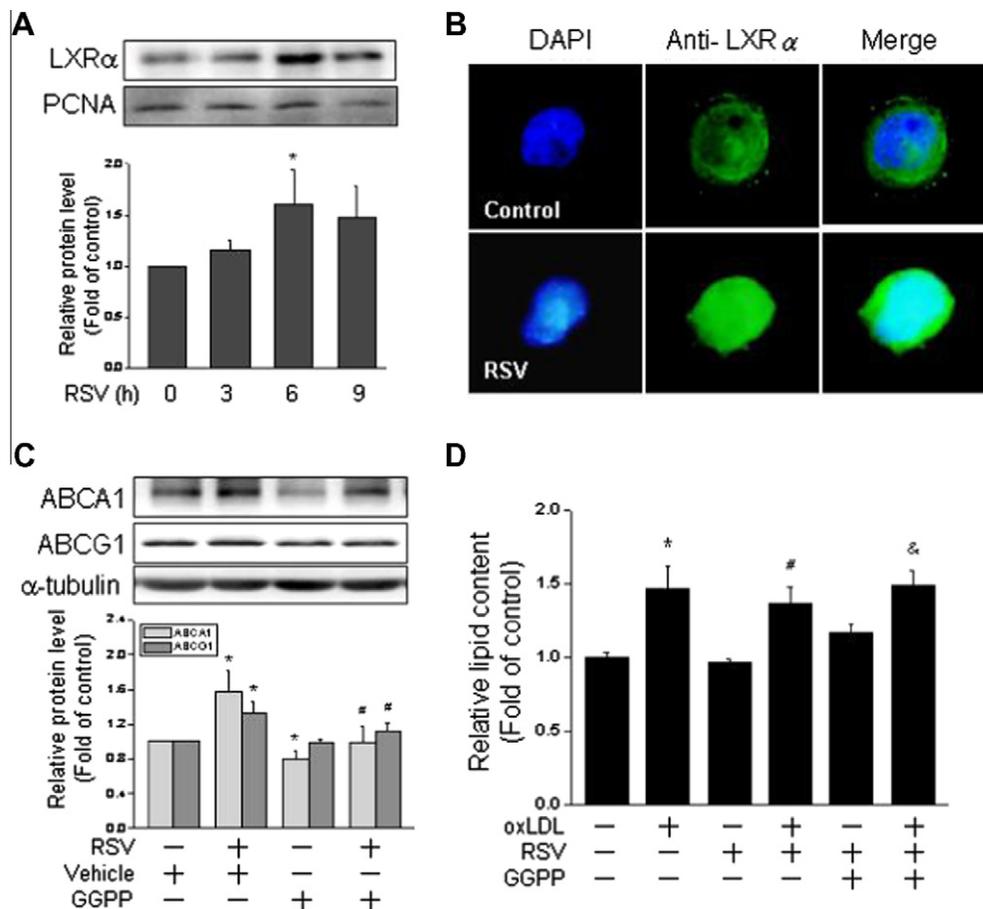
Fig. 5 – The role of LXRα in RSV-mediated gene expression of ABCA1 and ABCG1 and following lipid accumulation in THP-1-derived macrophages. (A) RSV increased LXRα protein levels. Macrophages were incubated with 20 μM RSV for the indicated time points (0–9 h), and the maximal expression of LXRα at 6 h. (B) RSV activated LXRα by promoting its nuclear translocation. Macrophages were treated with 20 μM RSV for 6 h (objective: 60×). (C) Inhibition of LXRα by GGPP abolished the expression of ABCA1 and ABCG1. Macrophages were pretreated with or without 20 μM GGPP for 2 h and then incubated with vehicle (DMSO) or RSV (20 μM) for another 16 h. (D) Inhibition of LXRα by GGPP affected RSV-attenuated lipid accumulation. After incubation with GGPP, macrophages were treated with vehicle (DMSO), RSV (20 μM), or RSV/oxLDL (50 μg/ml) for 24 h. The density of the lipid content was measured absorbance at 540 nm. Data are the mean ± SEM ($n = 8$). Statistical significance at [*]$P < 0.05$ compared with control; [#]$P < 0.05$ compared with RSV-treated alone; [&]$P < 0.05$ compared with RSV/oxLDL-treated group.

4.   Discussion

Emerging evidence suggests that RSV is a multifunctional antioxidant and provides *in vitro* and *in vivo* protection against CVD. The atheroprotective properties of RSV had been extensively investigated (Bhat et al., 2001; Bhavnani et al., 2001; Kaliora et al., 2006; Kopp, 1998; Renaud & de Lorgeril, 1992), and, although the precise mechanisms are not yet clear, the multifactorial, uncontrolled uptake of oxLDL or the dysregulation of cholesterol efflux in macrophages is thought to be the major contributor (Takahashi et al., 2002). In the present study, RSV inhibited oxLDL-mediated lipid accumulation through the enhancement of cholesterol efflux in THP-1-derived macrophages. Our data are in accordance with recent findings that RSV inhibited lipid peroxidation and promoted cholesterol efflux in mice macrophages (Berrougui et al., 2009). Based on this observation, we further elucidated the mechanisms underlying the

RSV-mediated suppression on the formation of foam cells. The intracellular cholesterol homeostasis in macrophages is dynamically regulated by the influx and efflux of cholesterol, processes that are tightly controlled by RCTs and SRs, respectively (Wang et al., 2004; Yokoyama, 2005). The data from this work demonstrated that RSV markedly upregulated the mRNA and protein expression of ABCA1 and ABCG1 in both dose- and time-dependent manners but that RSV increased the protein expression of SR-BI without affecting its mRNA expression. These results suggested that the enhancement of ABCA1 and ABCG1 by RSV might be regulated at the transcriptional level in human macrophages. The induction of SR-BI protein expression by RSV appeared to be the result of reduced protein degradation, but this requires further investigation. Our findings are consistent with the results of an *in vivo* study in mice that ABCA1 and ABCG1, but not SR-BI, promoted macrophage RCT (Wang et al., 2007).

It is well known that both *ABCA1* and *ABCG1* are target genes of the nuclear receptor, LXRα (liver X receptor), which is a key transcriptional factor in macrophages (Sevov et al., 2006). Our functional analyses indicated the inhibition of ABCA1 and ABCG1 by ABCA1 and ABCG1 shRNA, respectively, which demonstrated, at least in part, the beneficial effect of RSV against foam cell formation. We also showed that the upregulation of ABCA1 or ABCG1 reduced the oxLDL-induced lipid accumulation in foam cells via an LXRα-dependent mechanism. Furthermore, it was revealed that RSV activated LXRα by increasing its nuclear translocation, and the blockage of LXRα activation by GGPP diminished the RSV-mediated ABCA1 induction and consequently inhibited the accumulation of lipids. GGPP, however, had little effect on the ABCG1 level, implying a different regulatory mechanism underlying the RSV-mediated LXRα activation. Taken together, all of these results indicate the essential role of LXRα activation in the RSV-regulated gene expression of ABCA1 and ABCG1, contributing to the suppressive effects of RSV in foam cell transformation *in vitro*.

In addition to accumulating lipids, the foam cell release pro-inflammatory cytokines. Lipid-laden foam cell accumulation is a key feature of early stage atherosclerotic lesions because the pro-inflammatory factor affected cholesterol metabolism within vascular walls (Kleemann, Zadelaar, & Kooistra, 2008). These lipid-laden foam cells promoted inflammation in the vascular wall and induced monocyte CCR2 (CC-chemokine receptor 2) expression. The inhibitory effects of RSV on chemokine receptor binding and expression may contribute, in part, to affect the monocyte CCR2 binding activity in an NO-, MAPK- and PI3K-dependent manner in its cardiovascular protective activity *in vivo* (Cullen et al., 2007). The anti-oxidative activity and anti-inflammatory properties of RSV have been suggested to provide protection in CVD because RSV may directly or indirectly scavenge ROS (Bhat et al., 2001; Manna et al., 2000). Whether RSV may activate these signaling pathways related to antioxidant functions and, in turn, participate in the protective function against lipid accumulation via an LXRα-dependent mechanism in macrophages, requires further inquiry.

5. Conclusion

Our study demonstrated that the antiatherogenic properties of RSV ameliorated the oxLDL-mediated lipid accumulation in the process of lipid-laden foam cells formation via the upregulation of ABCA1 and ABCG1 in human macrophages. The upregulated expression of ABCA1 and ABCG1 by RSV was based on the transcriptional levels and was mediated by increasing the LXRα activity through the promotion of the nuclear translocation of LXRα. The ability of RSV to modulate the expression of the genes involved in cholesterol efflux suggested that polyphenols can potentially provide benefits on cholesterol homeostasis.

Conflict of interest

The authors declare no conflict of interest.

Acknowledgments

Appendix A. Supplementary data

Supplementary data associated with this article can be found, in the online version, at http://dx.doi.org/10.1016/j.jff.2012.04.012.

REFERENCES

Agarwal, B., & Baur, J. A. (2011). Resveratrol and life extension. *Annals of the New York Academy of Sciences, 1215*, 138–143.

Araya, J., Rodrigo, R., Orellana, M., & Rivera, G. (2001). Red wine raises plasma HDL and preserves long-chain polyunsaturated fatty acids in rat kidney and erythrocytes. *British Journal of Nutrition, 86*, 189–195.

Berrougui, H., Grenier, G., Loued, S., Drouin, G., & Khalil, A. (2009). A new insight into resveratrol as an atheroprotective compound: inhibition of lipid peroxidation and enhancement of cholesterol efflux. *Atherosclerosis, 207*, 420–427.

Bhat, K. P. L., Kosmeder, J. W., 2nd, & Pezzuto, J. M. (2001). Biological effects of resveratrol. *Antioxidants and Redox Signaling, 3*, 1041–1064.

Bhavnani, B. R., Cecutti, A., Gerulath, A., Woolever, A. C., & Berco, M. (2001). Comparison of the antioxidant effects of equine estrogens, red wine components, vitamin E, and probucol on low-density lipoprotein oxidation in postmenopausal women. *Menopause, 8*, 408–419.

Borra, M. T., Smith, B. C., & Denu, J. M. (2005). Mechanism of human SIRT1 activation by resveratrol. *Journal of Biological Chemistry, 280*, 17187–17195.

Chawla, A., Boisvert, W. A., Lee, C. H., Laffitte, B. A., Barak, Y., Joseph, S. B., Liao, D., Nagy, L., Edwards, P. A., Curtiss, L. K., Evans, R. M., & Tontonoz, P. (2001). A PPAR gamma-LXR-ABCA1 pathway in macrophages is involved in cholesterol efflux and atherogenesis. *Molecular Cell, 7*, 161–171.

Cuchel, M., & Rader, D. J. (2006). Macrophage reverse cholesterol transport: Key to the regression of atherosclerosis? *Circulation, 113*, 2548–2555.

Cullen, J. P., Morrow, D., Jin, Y., von Sweeney, N. O., Sitzmann, J. V., Cahill, P. A., & Redmond, E. M. (2007). Resveratrol inhibits expression and binding activity of the monocyte chemotactic protein-1 receptor, CCR2, on THP-1 monocytes. *Atherosclerosis, 195*, 125–133.

de Winther, M. P., & Hofker, M. H. (2000). Scavenging new insights into atherogenesis. *Journal of Clinical Investigation, 105*, 1039–1041.

Ferrero, M. E., Bertelli, A. E., Fulgenzi, A., Pellegatta, F., Corsi, M. M., Bonfrate, M., Ferrara, F., De Caterina, R., Giovannini, L., & Bertelli, A. (1998). Activity in vitro of resveratrol on granulocyte and monocyte adhesion to endothelium. *American Journal of Clinical Nutrition, 68*, 1208–1214.

Ji, Y., Jian, B., Wang, N., Moya-Sun, M. L., Phillips, M. C., Rothblat, G. H., Swaney, J. B., & Tall, A. R. (1997). Scavenger receptor BI promotes high density lipoprotein-mediated cellular cholesterol efflux. *Journal of Biological Chemistry, 272*, 20982–20985.

Kaliora, A. C., Dedoussis, G. V., & Schmidt, H. (2006). Dietary antioxidants in preventing atherogenesis. *Atherosclerosis, 187*, 1–17.

Kleemann, R., Zadelaar, S., & Kooistra, T. (2008). Cytokines and atherosclerosis: A comprehensive review of studies in mice. *Cardiovascular Research, 79*, 360–376.

Kopp, P. (1998). Resveratrol, a phytoestrogen found in red wine. A possible explanation for the conundrum of the 'French paradox'? *European Journal of Endocrinology, 138*, 619–620.

Li, A. C., & Glass, C. K. (2002). The macrophage foam cell as a target for therapeutic intervention. *Nature Medicine, 8*, 1235–1242.

Linsel-Nitschke, P., & Tall, A. R. (2005). HDL as a target in the treatment of atherosclerotic cardiovascular disease. *Nature Reviews Drug Discovery, 4*, 193–205.

Manna, S. K., Mukhopadhyay, A., & Aggarwal, B. B. (2000). Resveratrol suppresses TNF-induced activation of nuclear transcription factors NF-kappa B, activator protein-1, and apoptosis: potential role of reactive oxygen intermediates and lipid peroxidation. *Journal of Immunology, 164*, 6509–6519.

Ou, H. C., Chou, F. P., Sheen, H. M., Lin, T. M., Yang, C. H., & Sheu, H. H. (2006). Resveratrol, a polyphenolic compound in red wine, protects against oxidized LDL-induced cytotoxicity in endothelial cells. *Clinica Chimica Acta, 364*, 196–204.

Poussier, B., Cordova, A. C., Becquemin, J. P., & Sumpio, B. E. (2005). Resveratrol inhibits vascular smooth muscle cell proliferation and induces apoptosis. *Journal of Vascular Surgery, 42*, 1190–1197.

Renaud, S., & de Lorgeril, M. (1992). Wine, alcohol, platelets, and the French paradox for coronary heart disease. *Lancet, 339*, 1523–1526.

Sevov, M., Elfineh, L., & Cavelier, L. B. (2006). Resveratrol regulates the expression of LXR-alpha in human macrophages. *Biochemical and Biophysical Research Communications, 348*, 1047–1054.

Takahashi, K., Takeya, M., & Sakashita, N. (2002). Multifunctional roles of macrophages in the development and progression of atherosclerosis in humans and experimental animals. *Medical Electron Microscopy, 35*, 179–203.

Wallerath, T., Deckert, G., Ternes, T., Anderson, H., Li, H., Witte, K., & Förstermann, U. (2002). Resveratrol, a polyphenolic phytoalexin present in red wine, enhances expression and activity of endothelial nitric oxide synthase. *Circulation, 106*, 1652–1658.

Wang, X., Collins, H. L., Ranalletta, M., Fuki, I. V., Billheimer, J. T., Rothblat, G. H., Tall, A. R., & Rader, D. J. (2007). Macrophage ABCA1 and ABCG1, but not SR-BI, promote macrophage reverse cholesterol transport in vivo. *Journal of Clinical Investigation, 117*, 2216–2224.

Wang, N., Lan, D., Chen, W., Matsuura, F., & Tall, A. R. (2004). ATP-binding cassette transporters G1 and G4 mediate cellular cholesterol efflux to high-density lipoproteins. *Proceedings of the National Academy of Sciences of the United States of America, 101*, 9774–9779.

Wang, Z., Zou, J., Huang, Y., Cao, K., Xu, Y., & Wu, J. M. (2002). Effect of resveratrol on platelet aggregation in vivo and in vitro. *Chinese Medical Journal (English Edition), 115*, 378–380.

Yokoyama, S. (2005). Assembly of high density lipoprotein by the ABCA1/apolipoprotein pathway. *Current Opinion in Lipidology, 116*, 269–279.

Zhang, H., Morgan, B., Potter, B. J., Ma, L., Dellsperger, K. C., Ungvari, Z., & Zhang, C. (2010). Resveratrol improves left ventricular diastolic relaxation in type 2 diabetes by inhibiting oxidative/nitrative stress: In vivo demonstration with magnetic resonance imaging. *American Journal of Physiology – Heart and Circulatory Physiology, 299*, H985–H994.

Zou, J., Huang, Y., Chen, Q., Wei, E., Cao, K., & Joseph, M. W. (2000). Effects of resveratrol on oxidative modification of human low density lipoprotein. *Chinese Medical Journal (English Edition), 113*, 99–102.

Supplementary method

Determination of cytotoxicity

Before experiments, we pretest the effects of RSV on macrophages. THP-1 cells were first incubated with RSV for 16 h. At the end of the stimulation, mitochondrial dehydrogenase activity, which can be used as an index of cell viability, was assessed using the methylthiazoletetrazolium (MTT) assay. According to the results of MTT assay, we decided to use 20 μM as the working concentration of RSV.

Supplementary data

Suppl Table 1 Sequences used for the quantitative real-time PCR with optimized human ABCA1, ABCG1, SR-BI, and GAPDH-specific primer pairs.
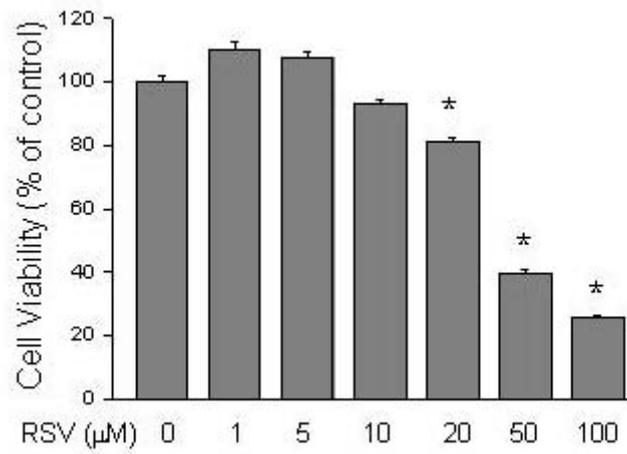
Gene	Forward	Reverse
ABCA1	CCAACAACCCCTGTTTCC	GCCTCCGAGCATCTGAGAAC
ABCG1	AGATTTTGTCATGGAGGTTGCA	TCACCCCCGAGGTCTCTCT
SR-BI	CTCCCATCCTCACTTCCTCAAC	CGTGACCGGGTGGATGTC
GAPDH	GACCTGGCCTACTGTGTGT	CAGCTTGCCTACAACTGAC

Supplementary figure legend

Suppl Fig. 1 Cytotoxicity of RSV on THP-1-derived macrophages. Macrophages were treated with the indicated concentrations of RSV (0-100 μM) for 16 h. Viability were determined by MTT assay. Data are the mean ± SEM (n = 4). Statistical significance at * P <0.05 compared with control.

Suppl Fig. 2 Determination of the shRNA clone suitable for the knowndown of ABCA1 or ABCG1 protein expression levels. Macrophages were transfected with 2 μg/ml shRNA against ABCA1 or ABCG1 for 24 h, respectively. The macrophages were transfected with the pLKO.1 plasmid in which random sequences were inserted as the experimental control. The cellular lysates were examined by western blot, and α-tubulin was used as the internal control. (A) The knockdown efficiency of five shRNA clones of ABCA1. Strain *e* was selected as the ABCA1 shRNA construct for the ensuing experiments. (B) The knockdown efficiency of five shRNA clones of ABCG1. Strain *d* was selected as the ABCG1 shRNA construct for the ensuing experiments. ABCA1 and ABCG1 shRNA inhibited the protein expression of ABCA1 and ABCG1 through specific knockdown.

Figure S1

Figure S2